Editors' Suggestion

Experimental Demonstration to Control the Pulse Length of Coherent Undulator Radiation by Chirped Microbunching

Takashi Tanaka,[1,*] Yuichiro Kida,[2] Satoshi Hashimoto,[3] Shuji Miyamoto,[3,†] Tadashi Togashi,[1,2] Hiromitsu Tomizawa,[1,2] Aoi Gocho,[4] Keisuke Kaneshima,[4] and Yoshihito Tanaka[4]

[1]*RIKEN SPring-8 Center, Koto 1-1-1, Sayo, Hyogo 679-5148, Japan*
[2]*Japan Synchrotron Radiation Research Institute, Koto 1-1-1, Sayo, Hyogo 679-5198, Japan*
[3]*Laboratory of Advanced Science and Technology for Industry, University of Hyogo, Koto 3-1-2, Kamigori, Hyogo 678-1205, Japan*
[4]*Graduate School of Science, University of Hyogo, Koto 3-2-1, Kamigori, Hyogo 678-1297, Japan*

(Received 23 June 2023; accepted 7 September 2023; published 3 October 2023)

In seeded free electron lasers (FELs), the temporal profile of FEL pulses usually reflects that of the seed pulse, and, thus, shorter FEL pulses are available with shorter seed pulses. In an extreme condition, however, this correlation is violated; the FEL pulse is stretched by the so-called slippage effect in undulators, when the seed pulse is ultimately short, e.g., few-cycles long. In a previous Letter, we have proposed a scheme to suppress the slippage effect and reduce the pulse length of FELs ultimately down to a single-cycle duration, which is based on "chirped microbunching," or an electron density modulation with a varying modulation period. Toward realization of FELs based on the proposed scheme, experiments have been carried out to demonstrate its fundamental mechanism in the NewSUBARU synchrotron radiation facility, using an ultrashort seed pulse with the pulse length shorter than five cycles. Experimental results of spectral and cross-correlation measurements have been found to be in reasonable agreement with the theoretical predictions, which strongly suggests the successful demonstration of the proposed scheme.

DOI: 10.1103/PhysRevLett.131.145001

Observation of ultrafast dynamics is an important research area in photon science, where intense and short-pulse laser sources play an important role; the laser pulse not only excites a target object, but also probes the transition of its state. In such pump-probe experiments, shortening the pulse lengths is the key to a better temporal resolution, and, thus, research and development to shorten the pulse length have been actively carried out in the field of laser engineering. Nowadays, intense ultrashort laser pulses are readily available in the infrared regions by means of the chirped pulse amplification technique, whose pulse length gets down to tens of femtoseconds with the peak power reaching a petawatt level; in addition, the pulse length can be further shortened by spectral broadening through nonlinear optical processes and compression by chirped mirrors. The high-power femtosecond pulses generated by such techniques can be also used to generate ultrashort pulses with the pulse length down to hundreds of attoseconds or shorter (attosecond pulses), by means of a high harmonic generation (HHG) process [1], where the femtosecond pulses are focused onto a gas medium and frequency up-converted to extreme-ultraviolet (EUV) regions. The HHG-based attosecond pulses have contributed to investigating ultrafast dynamics of electrons in matter [2], and their performances are being improved year by year [3]. Even so, attosecond pulse generation based on the HHG technique is still a great technical challenge, especially in terms of shortening the central wavelength for shorter pulse lengths. An alternative solution for attosecond pulses, which is known as a free electron laser (FEL) [4], is based on emission of coherent radiation from free electrons but not from bound electrons in atoms or molecules. Because a high-energy electron beam, moving in a periodically alternating magnetic field generated by a device called an undulator, works as a laser medium, no theoretical limit is present on the lasing wavelength in FELs; in fact, many FEL facilities are currently in operation in short-wavelength regions ranging from EUV to hard x-ray regions [5–11].

FELs operating in the short-wavelength regions can be classified into two types: self-amplified spontaneous emission (SASE) and seeded FELs. The former amplifies spontaneous radiation emitted by the electron beam itself, while the latter amplifies coherent light (seed pulse) generated by an external source and injected synchronously with the electron beam; note that the seed pulse can be also generated internally by the so-called self-seeding or cavity-based scheme [12,13].

Apart from technical difficulties, such as how to prepare short-wavelength coherent light and how to guarantee the temporal and spatial overlap between the electron beam and seed pulse, the seeded FELs are superior to the SASE FELs in terms of available photon flux and temporal coherence. In addition, the externally seeded FELs are

more advantageous for shortening the pulse lengths, because the temporal profile of FEL pulses usually reflects that of the seed pulse. As a result, we can take advantage of the ultrashort pulses available with the modern laser technologies to shorten the FEL pulse lengths. It should be noted, however, that the above discussion is not valid when an ultrashort seed pulse is used, which is of the order of few-cycles long. In such an extreme condition, the pulse length of seeded FELs is dominated by the number of undulator periods and can be much longer than that of the seed pulse; this comes from the slippage effect, in which radiation overtakes electrons by one wavelength in each undulator period. The pulse stretch driven by the slippage effect can be the biggest obstacle to shortening the FEL pulse with ultrashort seed pulses.

To overcome the difficulties mentioned above, we proposed a scheme to suppress the slippage effect in seeded FELs by means of "chirped microbunching" (CM) [14], which can potentially reduce the FEL pulse length down to a theoretical lower limit, i.e., single-cycle duration. After the first proposal, we and other groups have presented a number of ideas to take advantage of the CM scheme: generation of single-cycle terahertz radiation [15,16], further reducing the pulse length by synthesizing several harmonics [17] or by optimizing the magnetic field profile [18], application to high gain harmonic generation FELs [19] or Compton backscattering sources [20], and generation of isolated [21] and twin [22] attosecond pulses. Although all of them are attractive as new tools in photon science, suppressing the slippage effect by the CM scheme has not been demonstrated. Toward realization of CM-based light sources, we performed experiments to demonstrate the mechanism to suppress the slippage-driven pulse stretch and control the pulse length of coherent radiation.

The experiments were performed in an electron accelerator in the synchrotron radiation facility NewSUBARU [23] with an experimental setup schematically illustrated in Fig. 1; this is based on a scheme presented in [17,19] and is much simpler than the original one [14]. The accelerator is a racetrack storage ring with two long straight sections. During the demonstration experiments, it was operated in a single bunch mode, with the electron energy of 0.95 GeV, average beam current of 10 mA, full width at half maximum (FWHM) bunch length of 80 ps, natural emittance of 37 nm rad, coupling constant of 0.01, and energy spread of 4×10^{-4}.

In one of the two long straight sections (BL01), two identical undulators (modulator and radiator) have been installed together with a three-pole electromagnet as a chicane. The seed pulse is injected from the upstream side through the injection window. The electron beam interacts with the seed pulse in the modulator to induce an energy modulation, which is converted to a density modulation (microbunching) after passing through the chicane with the longitudinal dispersion of 50 μm. Then, the microbunched electron beam emits coherent radiation in the radiator, which is delivered to the diagnostics station located downstream of BL01.

A near-infrared laser source with the central wavelength of 800 nm has been installed in the upstream of BL01; to generate seed pulses short enough to demonstrate the CM scheme, we adopted a hollow fiber pulse compression scheme [24]. By focusing part of the femtosecond laser pulse from a Ti:sapphire regenerative amplifier into a hollow fiber (length of 0.5 m and core diameter of 250 μm) filled with Ar gas (pressure of 0.4 atm), a broadband laser pulse ranging from 700 to 900 nm is generated, with a pulse energy of 0.12 mJ; note that this is slightly lower than 0.15 mJ, the pulse energy without applying the hollow fiber scheme, i.e., without Ar gas. Because of Fresnel loss at the injection window, the pulse energy actually delivered to the modulator is about 0.1 (0.13) mJ with (without) the Ar gas.

Because the broadband pulse generated by the hollow fiber scheme is chirped, it should be compressed by chirped mirrors before delivering to the modulator. Note that the pulse should pass through a few dispersive media before

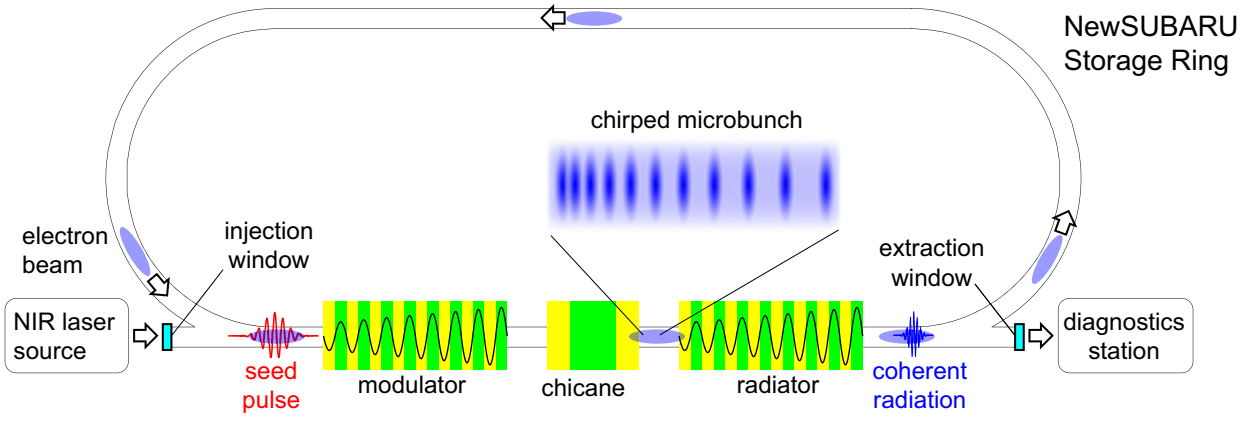

FIG. 1. Experimental setup to demonstrate the CM scheme.

injection to the storage ring, such as air in the 10-m-long transport line and glass in the injection window to secure the storage ring vacuum. Thus, the chirped mirrors have been optimized so that the broadband pulse becomes transform limited when it arrives at the center of the modulator, considering the dispersion in the injection transport line. Because it is impossible to measure the pulse length exactly there, we built a virtual transport line composed of identical elements and confirmed that the seed pulse at the virtual modulator was transform limited, by means of a frequency-resolved optical gating method.

Another important point in the seed pulse is the spatial matching with the electron beam. Ideally, the pulse should interact with the electron beam uniformly along the whole modulator. Considering the FWHM electron beam size of 1.2 (0.14) mm in the horizontal (vertical) direction, the optics in the transport line has been designed so that the seed pulse is focused at the middle of the modulator with the waist size of ∼1.5 mm.

The trigger signal, which drives the seed laser system and determines its timing with respect to the electron beam, is generated by frequency dividing and up-converting the master oscillator signal driving the radio-frequency accelerator cavity of the storage ring. The timing jitter between the seed pulse and electron beam measured by a 16-GHz oscilloscope was 7.1 ps and well below the electron bunch length.

Each undulator is 3.84 m long with the magnetic period of 160 mm and, thus, has 24 periods. The minimum gap is 45 mm with the maximum field amplitude of 0.68 T. To adjust the field gradient of the modulator and radiator flexibly to perform the demonstration experiments, the undulator is equipped with a function to adjust the magnet gap independently at each period [25]. As a result, the longitudinal profile of the magnetic field can be arbitrarily varied, which means that not only the field gradient, but also the number of effective periods can be controlled by intentionally detuning several periods. In the normal condition, the modulator (radiator) is tuned to generate a constant field of 0.55 (0.38) T without the field gradient. Then the electron beam interacts with the seed pulse (800 nm) and generates coherent radiation with the wavelength of 400 nm.

The diagnostics station located downstream of BL01 is composed of three elements: position monitor, timing monitor, and cross-correlator. They characterize not only the spontaneous and coherent radiation emitted by the electron beam, but also the seed pulse transported through BL01.

The position monitor is composed of a biconvex lens, bandpass filter (800 nm), and CMOS camera and plays a role to guarantee the spatial overlap between the electron beam and seed pulse at the modulator. The focal image of spontaneous radiation gives the information on the transverse position of the electron beam relative to the seed pulse at the modulator. Once the positional difference is detected, the injection condition of the seed pulse is adjusted; the electron beam trajectory was fixed so as not to disturb the storage ring operation.

The timing monitor is composed of a focusing lens, diffraction grating, and streak camera and measures the temporal profiles of spontaneous radiation emitted at the modulator as well as the arrival timings of the seed pulse, both of which have the central wavelength of 800 nm. The results are then used to tune the trigger signal to guarantee the temporal overlap between the electron beam and seed pulse. Another important role of this system is to measure time-resolved spectra of coherent and spontaneous radiation emitted at the radiator, with the central wavelength of 400 nm. Note that the temporal resolution of the streak camera is around 1 ps, and, thus, the pulse length of coherent radiation, which is supposed to be shorter than 100 fs, cannot be directly measured.

The cross-correlator evaluates the pulse length of coherent radiation, in which a 10-μm-thick β-BaB_2O_4 crystal is used for sum-frequency generation (SFG) between the seed pulse and coherent radiation. The seed pulse length can be also evaluated by an autocorrelation measurement with the same setup.

We first measured the spectra of seed pulses with and without the hollow fiber scheme. The results are shown in Fig. 2, where we find that the bandwidth of the former is about 4 times broader than the latter. To facilitate the following discussions, let us call the former and latter conditions broadband and narrow-band ones. The FWHM pulse lengths measured at the virtual modulator by an autocorrelation method were 12 and 48 fs for the broadband and narrow-band conditions, respectively. Namely, the seed pulse is compressed from 18 cycles to 4.5 cycles by the hollow fiber scheme.

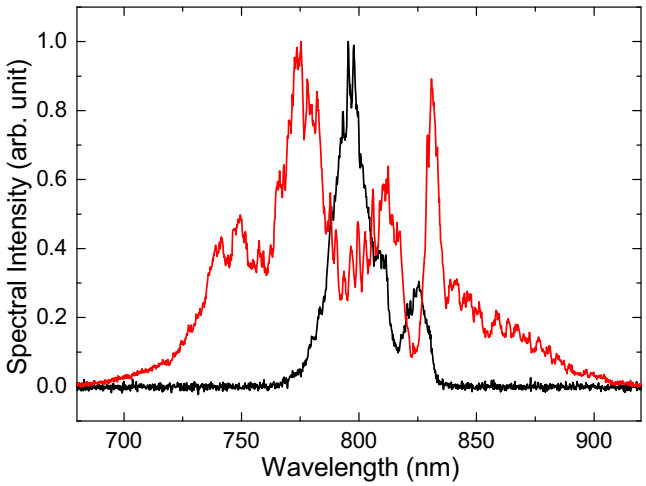

FIG. 2. Measured spectra of the seed pulse with (red line) and without (black line) the hollow fiber pulse compression scheme.

TABLE I. Conditions of the seed pulse and undulators for the spectral measurements.

Condition	Seed pulse	N_{eff}	dB/dz
(i)	Narrow-band	24	0
(ii)	Broadband	24	0
(iii)	Broadband	12	0
(iv)	Broadband	6	0
(v)	Broadband	24	2.9%/m
(vi)	Narrow-band	24	2.9%/m

To demonstrate the CM scheme, we measured spectra of coherent radiation under six different conditions defined by three parameters summarized in Table I: the seed pulse (narrow-band or broadband), effective number of undulator periods ($N_{\mathrm{eff}} = 24$, 12, or 6), and undulator field gradient dB/dz (0 or 2.9%/m). Note that the modulator and radiator have the same parameters (N_{eff} and dB/dz) in each condition, except for the average peak field. Among these conditions, the CM scheme was examined in (v) using the broadband seed pulse with tapered undulators.

The spectral measurement has been done using the timing monitor, i.e., the diffraction grating and streak camera; we took 100 shots of time-resolved spectra in each condition and averaged over the whole shots after correcting the timing jitter of the streak camera. Then we summed up the data contained in a limited time window corresponding to the coherent radiation to reduce the contribution from spontaneous radiation and background.

We first mention the general properties of coherent radiation generated in condition (i). The peak power evaluated from the measured temporal profile was at least 4 orders of magnitude higher than that of spontaneous radiation. The pulse energy measured by an optical power meter was around 1 nJ, which is well consistent with a theoretical prediction. The spectral profile was stable during the measurement, and shot-to-shot fluctuation was small.

Figure 3(a) shows the spectral measurement results with the Roman numbers in the legend indicating the experimental conditions in Table I. Note that the vertical scale is varied according to the condition to facilitate visualization.

The black line shows the result with the narrow-band seed pulse (i), in which case coherent radiation with a narrow bandwidth of ~5 nm is generated. This is consistent with an assumption that the seed pulse with the pulse length of 48 fs generates coherent radiation with the same pulse length. If this assumption can be applied to the broadband seed pulse as well, coherent radiation with the pulse length of 12 fs is generated. Then the bandwidth is expected to be 20 nm; in practice, this is not valid as shown in the red line (ii), where we find a much narrower bandwidth of ~7 nm,

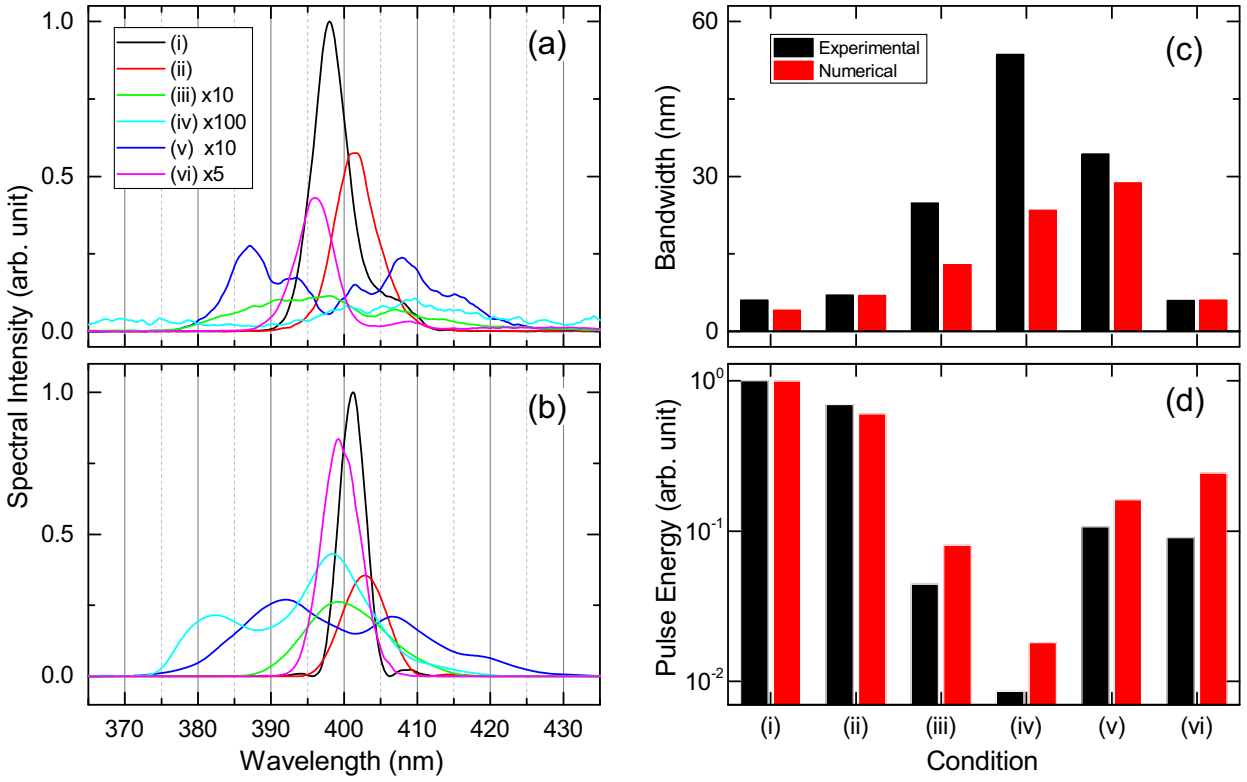

FIG. 3. Experimental results of spectral measurement under the six conditions (i)–(vi) summarized in Table I and comparison with theoretical results: (a) measured and (b) computed spectra and (c),(d) FWHM bandwidth and pulse energy evaluated by Gaussian fitting of each spectrum.

and, thus, the pulse length must be much longer than 12 fs. The discrepancy obviously comes from the slippage-driven pulse stretch.

One simple solution toward shorter pulse lengths (and, thus, broader spectra) is to reduce the number of undulator periods, which is examined in conditions (iii) and (iv), whose experimental results are shown in the green and cyan lines. Although the bandwidth becomes broader for fewer undulator periods, the intensity of coherent radiation drastically drops. This is the reason why we have proposed the CM scheme as a realistic solution to suppressing the slippage effect.

To demonstrate the CM scheme, we examined condition (v) in which the modulator and radiator are tapered with the same field gradient of 2.9%/m instead of reducing the undulator periods; note that the gradient was optimized in advance, by measuring the intensity of coherent radiation with the modulator and radiator being detuned and evaluating the acceptable field variation of them. To be more specific, applying a larger field gradient does not broaden the bandwidth but decreases the intensity. The blue line shows the experimental result, where we find that the bandwidth is much broader than that without the taper (ii), and the intensity is much higher than that with fewer undulator periods [(iii) and (iv)], suggesting that the CM scheme works in this condition to control the pulse length of coherent radiation. This is not the case in condition (vi), where the narrow-band seed pulse cannot induce the CM; instead, it induces regular (nonchirped) microbunching regardless of the undulator parameter. As a result, tapering the undulator just results in the reduction of spectral intensity without broadening the spectrum.

To verify the validity of the experimental results, we numerically evaluated the spectra predicted in the respective conditions using the simulation code SPECTRA [26]; the results are plotted in Fig. 3(b), where we find a reasonable agreement between the experimental and numerical results. For a more quantitative comparison, we carried out Gaussian fitting of the experimental and numerical spectra to retrieve the bandwidth and pulse energy in each condition, which are plotted in Figs. 3(c) and 3(d); the experimental results are consistent with the numerical ones, albeit larger discrepancies (bandwidth and intensity) are found in the fewer period conditions [(iii) and (iv)]. This may be attributable to other factors not taken into account in the numerical evaluation (pointing stability of the seed pulse, etc.). Under the fewer period condition where the interaction between the electron beam and seed pulse is weaker, the spectrum can be more sensitive to the above factors that can spoil the process of coherent radiation.

The experimental and numerical results presented above, in particular, under the conditions without (ii) and with (v) the undulator tapering, suggests the effectiveness of the CM scheme. To strengthen the experimental demonstration of the CM scheme further, we performed cross-correlation measurements in these conditions. The results are shown in Fig. 4 together with numerical predictions, in which both results are normalized by the maximum signal in condition (ii). The experimental results are in good agreement with the numerical ones in both conditions, except for several data points in (v); this is probably attributable to intensity fluctuation of coherent radiation during the measurement.

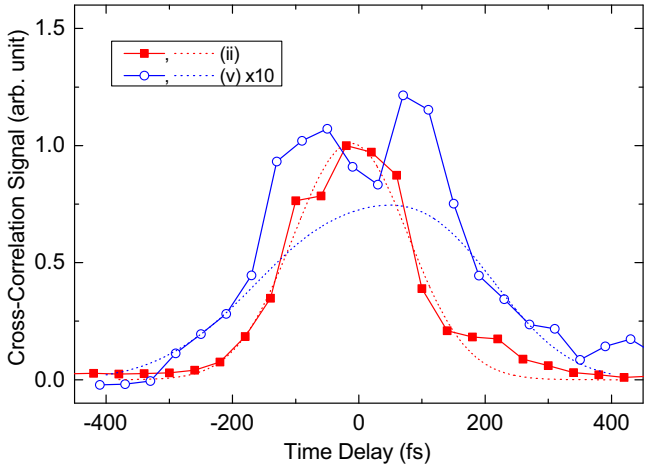

FIG. 4. Cross-correlation measurement for SFG signal between the seed pulse and coherent radiation, with (blue circles) and without (red squares) the CM scheme. The dashes lines show numerical predictions in the same conditions.

The consistency between the experimental and numerical results presented above proves the validity of the experimental setup and procedure, as well as the numerical methods.

Finally, let us discuss the pulse length of coherent radiation with and without the CM scheme. It should be noted that the coherent radiation generated at the radiator is easily stretched by the dispersive media in the transport line, and, thus, the pulse length at the diagnostics station is much longer than the original one at the radiator. For example, the original pulse lengths with and without the CM scheme predicted by the numerical method are 12 and 48 fs, which are stretched to 350 and 84 fs at the diagnostics station because of the dispersion in the transport line (air and glass of the extraction window, whose group delay dispersions are 500 and 575 fs^2, respectively). Thus, deducing the original pulse length experimentally, in particular, that with the CM scheme, involves a great deal of uncertainty. Even so, what was observed in this Letter can be reasonably explained by the fundamental mechanism of the CM scheme, namely, suppressing the slippage-driven pulse stretch of coherent undulator radiation.

The experimental demonstration of the CM scheme definitely accelerates its realization toward practical applications; in particular, waveform-controlled twin attosecond pulses that can be generated by applying the CM scheme [21,22] provide a novel tool in photon science, such as pump-probe experiments with an unprecedented temporal resolution.

This work was supported by JSPS KAKENHI Grant No. 18H03691.

*ztanaka@spring8.or.jp
†Present address: Institute of Laser Engineering, Osaka University, Osaka 565-0871, Japan.

[1] F. Krausz and M. Ivanov, Rev. Mod. Phys. **81**, 163 (2009).
[2] G. Sansone, L. Poletto, and M. Nisoli, Nat. Photonics **5**, 655 (2011).
[3] J. Li, J. Lu, A. Chew, S. Han, J. Li, Y. Wu, H. Wang, S. Ghimire, and Z. Chang, Nat. Commun. **11**, 2748 (2020).
[4] B. W. J. McNeil and N. R. Thompson, Nat. Photonics **4**, 814 (2010).
[5] W. Ackermann *et al.*, Nat. Photonics **1**, 336 (2007).
[6] P. Emma *et al.*, Nat. Photonics **4**, 641 (2010).
[7] T. Ishikawa *et al.*, Nat. Photonics **6**, 540 (2012).
[8] E. Allaria *et al.*, Nat. Photonics **6**, 699 (2012).
[9] H.-S. Kang *et al.*, Nat. Photonics **11**, 708 (2017).
[10] E. Prat *et al.*, Nat. Photonics **14**, 748 (2020).
[11] W. Decking *et al.*, Nat. Photonics **14**, 391 (2020).
[12] J. Amann *et al.*, Nat. Photonics **6**, 693 (2012).
[13] K.-J. Kim, Y. Shvyd'ko, and S. Reiche, Phys. Rev. Lett. **100**, 244802 (2008).
[14] T. Tanaka, Phys. Rev. Lett. **114**, 044801 (2015).
[15] T. Tanaka, Opt. Lett. **43**, 4485 (2018).
[16] H. Zhang, W. Wang, S. Jiang, C. Li, Z. He, Q. Jia, L. Wang, and D. He, Phys. Rev. Accel. Beams **23**, 020704 (2020).
[17] Y. Kida, R. Kinjo, and T. Tanaka, Appl, Phys. Lett. **109**, 151107 (2016).
[18] V. A. Goryashko, Phys. Rev. Accel. Beams **20**, 080703 (2017).
[19] T. Tanaka and P. R. Ribič, Opt. Express **27**, 30875 (2019).
[20] B. H. Schaap, P. W. Smorenburg, and O. J. Luiten, Sci. Rep. **12**, 19727 (2022).
[21] P. R. Ribič and T. Tanaka, Opt. Lett. **45**, 5234 (2020).
[22] T. Tanaka and P. R. Ribič, Opt. Lett. **47**, 1411 (2022).
[23] A. Ando, S. Amano, S. Hashimoto, H. Kinosita, S. Miyamoto, T. Mochizuki, M. Niibe, Y. Shoji, M. Terasawa, T. Watanabe, and N. Kumagai, J. Synchrotron Radiat. **5**, 342 (1998).
[24] S. Sartania, Z. Cheng, M. Lenzner, G. Tempea, C. Spielmann, F. Krausz, and K. Ferencz, Opt. Lett. **22**, 1562 (1997).
[25] T. Tanaka, Y. Kida, R. Kinjo, T. Togashi, H. Tomizawa, S. Hashimoto, S. Miyamoto, S. Okabe, and Y. Tanaka, J. Synchrotron Radiat. **28**, 404 (2021).
[26] T. Tanaka, J. Synchrotron Radiat. **28**, 1267 (2021).